Molecular behaviour of elastomeric materials under large deformation: 1. Re-evaluation of the Mooney–Rivlin plot

Yoshihide Fukahori and Wataru Seki
Research and Development Division, Bridgestone Corporation, Kodaira-Shi, Tokyo 187, Japan
(Received 30 November 1990; accepted 7 January 1991)

Partial derivatives of the strain energy function $\partial W/\partial I_1$ and $\partial W/\partial I_2$ are widely evaluated for various rubber vlucanizates under small to very large extension. The Mooney–Rivlin plot is reproduced with the plot of the original equation, $\sigma = 2(\lambda - \lambda^{-2})\ (\partial W/\partial I_1 + \lambda^{-1}\partial W/\partial I_2)$, in which an inevitability for the plot to give a straight line is not found. Even if a straight line is obtained, the constants C_1 and C_2 differ from $\partial W/\partial I_1$ and $\partial W/\partial I_2$, respectively.

(Keywords: rubber vulcanizates; stress–strain relation; Mooney–Rivlin plot; strain energy function; large deformation)

INTRODUCTION

In recent rubber engineering and technology, computer techniques (particularly finite element analysis) have been widely applied to stress analysis and design of structures, expanding its boundary from small to considerably large deformation. The most important point required in such fields, of course, is the accuracy of the computation which strictly depends on how accurate information can be introduced concerning characteristics of materials, the strain energy function of the material applicable for a wide range and mode of deformation.

In a phenomenological approach of rubber elasticity theories, the well-known Mooney–Rivlin strain energy function is the most widely investigated constitutive relationship in stress–strain analysis of rubber-like materials. The semi-empirical Mooney–Rivlin plot has been the subject of many studies because of its simplicity and the expectation that it can show the stress–strain behaviour of rubber-like materials at medium deformation. In addition, there have also been many attempts to assign a molecular mechanism to the Mooney constants, although the Mooney–Rivlin approach is not based on a molecular model.

In this paper, we first evaluate and characterize the strain energy function of various rubber vulcanizates with a newly designed apparatus which can perform under small to large, and particularly up to very large deformation. Subsequently, the Mooney–Rivlin plots for simple extension are compared with those derived from its original equation theoretically and experimentally. We discuss why a straight line does appear on the Mooney–Rivlin plot.

THEORETICAL BACKGROUND

Considering the continuum theory of finite deformation, the stress–strain equation of homogeneous, isotropic and elastic materials such as vulcanized rubber can be derived from the strain energy function (more precisely, the strain energy density function) W, where W is the elastic energy stored in a deformed body. According to Rivlin[1], the strain energy function W is given as a function of strain invariants I_1, I_2 and I_3:

$$W = W(I_1, I_2, I_3) \tag{1}$$

where

$$I_1 = \lambda_1^2 + \lambda_2^2 + \lambda_3^2 \tag{2}$$

$$I_2 = \lambda_1^2\lambda_2^2 + \lambda_2^2\lambda_3^2 + \lambda_3^2\lambda_1^2 \tag{3}$$

$$I_3 = \lambda_1^2\lambda_2^2\lambda_3^2 \tag{4}$$

and λ_1, λ_2 and λ_3 are the principal extension ratios. In general, the third invariant becomes unity ($I_3 = 1$) because of the incompressibility of rubber. Thus W is given as a function of I_1 and I_2.

Now, considering a homogeneous biaxial deformation, the principal stresses (engineering stresses) σ_1 and σ_2 are derived[2] from W:

$$\sigma_1 = \frac{2}{\lambda_1}\left(\lambda_1^2 - \frac{1}{\lambda_1^2\lambda_2^2}\right)\left(\frac{\partial W}{\partial I_1} + \lambda_2^2\frac{\partial W}{\partial I_2}\right) \tag{5}$$

$$\sigma_2 = \frac{2}{\lambda_2}\left(\lambda_2^2 - \frac{1}{\lambda_1^2\lambda_2^2}\right)\left(\frac{\partial W}{\partial I_1} + \lambda_1^2\frac{\partial W}{\partial I_2}\right) \tag{6}$$

Then $\partial W/\partial I_1$ and $\partial W/\partial I_2$ can be given by substituting the data sets of σ_1, σ_2 and the corresponding λ_1, λ_2 into the following equations derived from equations (5) and (6):

$$\frac{\partial W}{\partial I_1} = \frac{1}{2(\lambda_1^2 - \lambda_2^2)}\left(\frac{\lambda_1^3\sigma_1}{\lambda_1^2 - \lambda_1^{-2}\lambda_2^{-2}} - \frac{\lambda_2^3\sigma_2}{\lambda_2^2 - \lambda_1^{-2}\lambda_2^{-2}}\right) \tag{7}$$

$$\frac{\partial W}{\partial I_2} = \frac{1}{2(\lambda_2^2 - \lambda_1^2)}\left(\frac{\lambda_1\sigma_1}{\lambda_1^2 - \lambda_1^{-2}\lambda_2^{-2}} - \frac{\lambda_2\sigma_2}{\lambda_2^2 - \lambda_1^{-2}\lambda_2^{-2}}\right) \tag{8}$$

0032-3861/92/030502-07

In the case of uniaxial extension, considering $\lambda_2 = \lambda_1^{-1/2}$

$$\sigma = 2(\lambda - \lambda^{-2})\left(\frac{\partial W}{\partial I_1} + \lambda^{-1}\frac{\partial W}{\partial I_2}\right) \quad (9)$$

The mathematically general form of W for an isotropic and incompressible material is given[3] as:

$$W = \sum_{i,j}^{\infty} C_{ij}(I_1 - 3)\,(I_2 - 3) \quad (10)$$

The lowest formula of series ($i = 1, j = 0$) is functionally identical to the classical Gaussian theory of rubber elasticity[4] ($C_1 = C_{10}$)

$$W = C_1(I_1 - 3) \quad (11)$$

Then, $\partial W/\partial I_1 = C_1$, $\partial W/\partial I_2 = 0$ and

$$\sigma = \frac{\partial W}{\partial \lambda} = 2C_1(\lambda - \lambda^{-2}) \quad (12)$$

Rivlin and Saunders[5] proposed an equation of higher order expression through their biaxial testing:

$$W = C_1(I_1 - 3) + C_2(I_2 - 3) \quad (13)$$

where C_1 and C_2 are constants, then $\partial W/\partial I_1 = C_1$ and $\partial W/\partial I_2 = C_2$. For unaxial extension, equation (13) gives:

$$\sigma = 2(\lambda - \lambda^{-2})\,(C_1 + \lambda^{-1}C_2) \quad (14)$$

Equation (14) is the Mooney–Rivlin equation and identical to equatin (9). Then if C_1 and C_2 are actually constants, as would be expected, C_1 and C_2 can be determined with the so-called Mooney–Rivlin plot through uniaxial extension testing, i.e. the plot of $\sigma/2(\lambda - \lambda^{-2})$ against λ^{-1}. C_1 and C_2 thus obtained were regarded to give the general parameters $\partial W/\partial I_1$ and $\partial W/\partial I_2$, respectively, at medium deformation, although such a plot for real rubber vulcanizates deviates from a straight line at small and large deformation. It should be restated again, however, that this procedure is valid only when both parameters C_1 and C_2 in equation (14), then $\partial W/\partial I_1$ and $\partial W/\partial I_2$ in equation (9), are contants. Conversely speaking, even if there appears to be a straight line in the plot, it does not necessarily mean that both parameters are constants. For example, if $\partial W/\partial I_1 = a/\lambda$ and $\partial W/\partial I_2 = b\lambda$ and a, b are constants, the plot will also give a straight line. It is fundamentally impossible to decide two unknown parameters $\partial W/\partial I_1$ and $\partial W/\partial I_2$ with equations (9) or (14), or in other words, with simple extension testing. As Kawabata *et al.*[6] showed experimentally, $\partial W/\partial I_1$ and $\partial W/\partial I_2$ are complicated functions of I_1 and I_2 then λ_1 and λ_2, therefore it is quite important to evaluate the Mooney–Rivlin plot tracing back to its original equation, equation (9).

EXPERIMENTS

Apparatus

New apparatus was designed to perform strip biaxial (pure shear) testing (*Figure 1*). Both edges of the rectangular test piece were thicker than the central part to avoid fracture or slippage of the clamped edges. The test piece can be extended freely to $\lambda_1 = 6.0$ in the x-direction, while in the y-direction it is kept constant ($\lambda_2 = 1$) by being gripped in sliding clamps. Thus, the data σ_1 and σ_2 measured by paired load cells connected to fixed crossheads make calculations of $\partial W/\partial I_1$ and $\partial W/\partial I_2$ from equations (7) and (8) possible. *Figure 2* shows that the lattice printed on the test piece is held in the pure shear state even under high extension. Experiments were performed at crosshead speeds of 50 mm min^{-1} at room temperature (24°C) both in strip biaxial and uniaxial extension. The constants C_1 and C_2 were given as the intercept at $\lambda^{-1} = 0$ and the slope of a straight line in the Mooney–Rivlin plot, respectively.

Materials

The materials studied here were natural rubber vulcanizates (NR1–NR3), carbon black reinforced natural rubber vulcanizates (NR4–NR7) and other vulcanizates of butadiene rubber (BR), styrene butadiene rubber (SBR) and nitrile butadiene rubber (NBR). The relevant compounding details are given in *Table 1*.

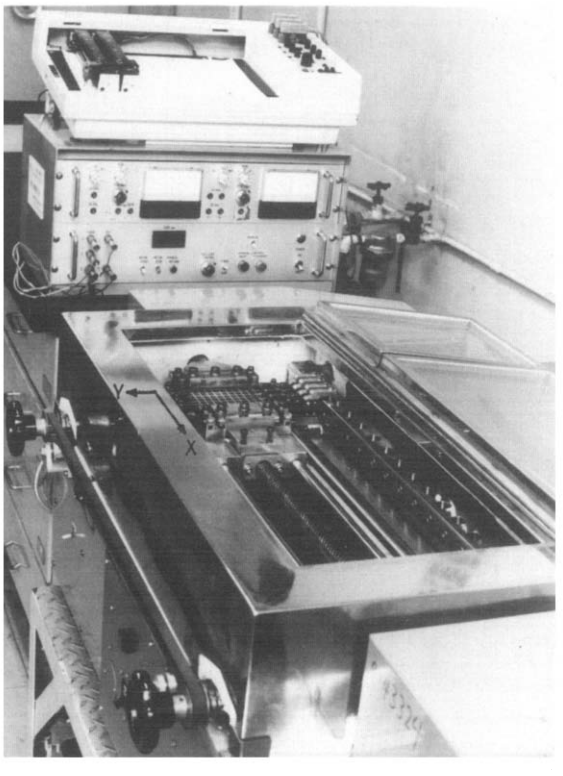

Figure 1 The strip biaxial testing machine

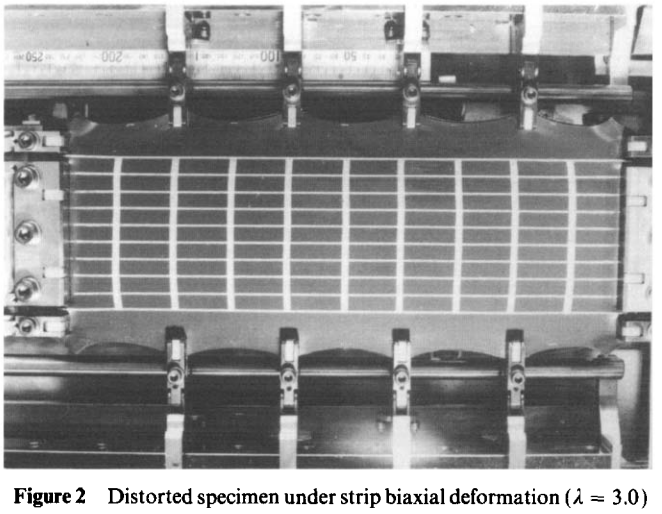

Figure 2 Distorted specimen under strip biaxial deformation ($\lambda = 3.0$)

Table 1 Compounding details of the materials (parts by weight)

Composition	NR1	NR2	NR3	NR4	NR5	NR6	NR7	BR	SBR	NBR
Rubber	100 (NR)	←	←	←	←	←	←	100 (BR)	100 (SBR)	100 (NBR)
Carbon black	0	0	0	20 (HAF)	25 (FT)	40 (HAF)	60 (HAF)	0	0	0
Sulphur	0.7	2.0	5.0	2.0	1.5	2.0	2.0	1.5	1.5	1.5

In addition, zinc oxide (5.0) and steric acid (2.0) for all rubbers and aromatic oil (9.0) for NR5 only

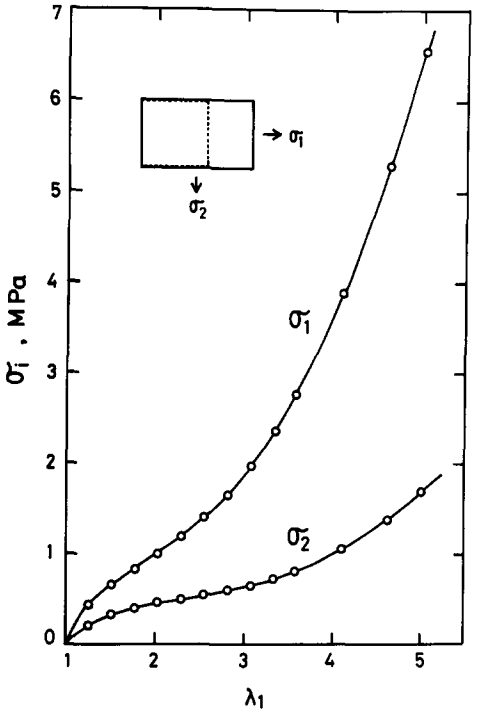

Figure 3 Stress–extention ratio relations under strip biaxial conditions

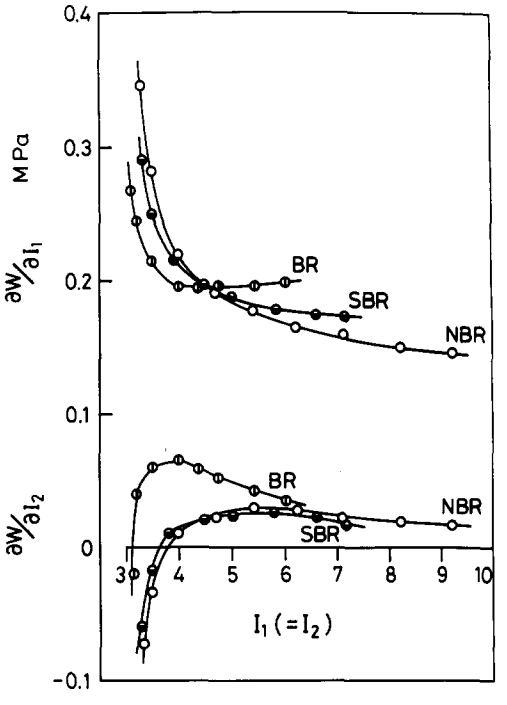

Figure 4 $\partial W/\partial I_1$ and $\partial W/\partial I_2$ as a function of I_1

RESULTS AND DISCUSSION

Characteristics of the strain energy function of rubber vulcanizates

The stresses σ_1 and σ_2 of NR5 obtained in strip biaxial testing are shown in *Figure 3* as a function of the principal extension ratio λ_1, where σ_1, λ_1 and σ_2, $\lambda_2(=1)$ correspond to the x and y directions, respectively. The values of $\partial W/\partial I_1$ and $\partial W/\partial I_2$ for all materials calculated using equations (7) and (8) are plotted against strain invariant I_1 ($=I_2$ in strip biaxial) in *Figures 4–6*. As Kawabata *et al.*[6] indicated, $\partial W/\partial I_1$ and $\partial W/\partial I_2$ are not contant but have typical features varying with strain invariant I_1. Virtually all of the rubber vulcanizates, filled and unfilled, have similar features. That is, $\partial W/\partial I_1$ decreases rapidly with increasing I_1 and has a minimum value in a region of small invariant $I_1 = 3$–6, following which $\partial W/\partial I_1$ increases again with increasing I_1. In contrast, $\partial W/\partial I_2$ increases rapidly at first, then decreases gradually after passing the maximum with increasing I_1.

Figure 4 shows the $\partial W/\partial I_1$–I_1 and the $\partial W/\partial I_2$–I_1 curves of various gum vulcanizates, which only give results measured at small invariant I_1 because of their poor tensile properties under biaxial deformation. *Figure 5* shows how $\partial W/\partial I_1$ and $\partial W/\partial I_2$ vary with the amount of vulcanizing agent, sulphur, in unfilled NR.

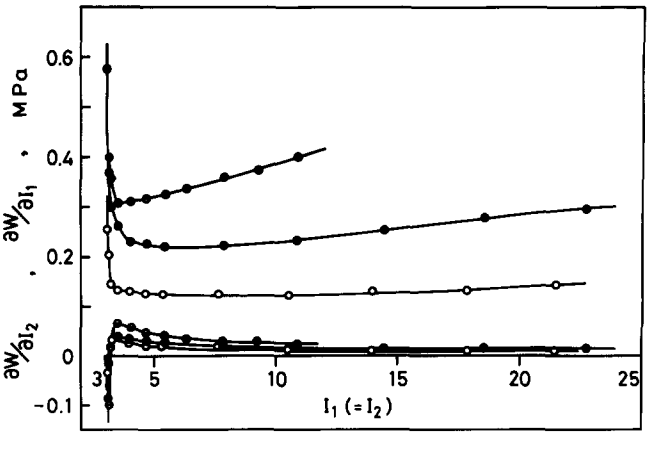

Figure 5 As in *Figure 4*: (○) NR1; (⊙) NR2; (⊖) NR3

The term $\partial W/\partial I_1$ increases in absolute value and in its positive slope and $\partial W/\partial I_2$ also increases slightly with increasing sulphur content. It is clearly seen that $\partial W/\partial I_1$ of gum vulcanizates with a normal amount of vulcanizing agent is nearly constant at medium deformation, the ratio of $\partial W/\partial I_2$ to $\partial W/\partial I_1$ being 1/5–1/10.

In filled NR vulcanizates, however, $\partial W/\partial I_1$ is not constant. *Figure 6* shows that the value increases greatly

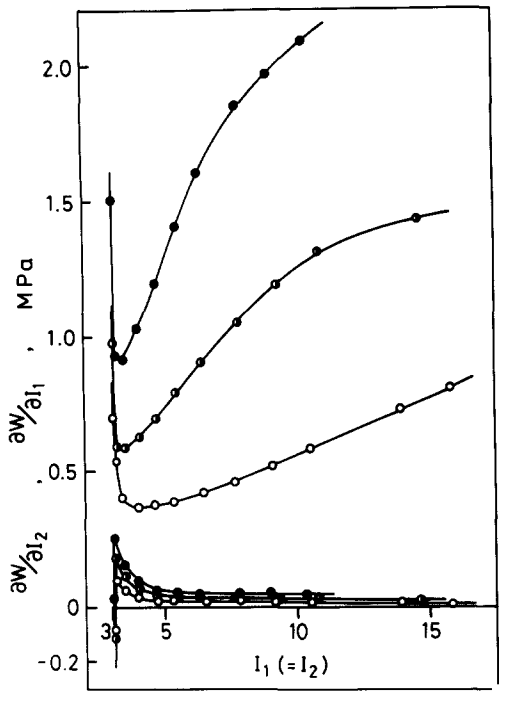

Figure 6 As in *Figure 4*: (○) NR4; (◑) NR6; (●) NR7

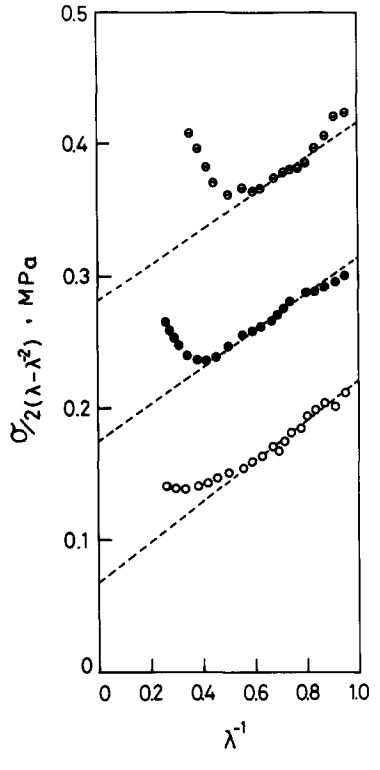

Figure 7 Mooney–Rivlin plots: (○) NR1; (⊙) NR2; (⊖) NR3

with increasing carbon black, in particular, the positive slope of the curves becomes steeper. $\partial W/\partial I_2$ also increases with increasing filler content but is negligible compared with $\partial W/\partial I_1$.

The Mooney–Rivlin plot of rubber vulcanizates

Why does the Mooney–Rivlin plot give a straight line for materials for which $\partial W/\partial I_1$ and $\partial W/\partial I_2$ are not constant but a complicated function of λ? We shall evaluate the Mooney–Rivlin equation, equation (14), comparing it with equation (9) using the empirical data of $\partial W/\partial I_1$ and $\partial W/\partial I_2$ obtained for real rubber vulcanizates. Here, we set up the reduced stress $\sigma^* = \sigma/2(\lambda - \lambda^{-2})$. *Figures 7* and *8* are the Mooney–Rivlin relation plotted with data obtained in uniaxial extension for unfilled and filled NR, respectively. Something similar to straight lines with positive slope are seen in *Figure 7*, and can also be detected in *Figure 8*. From a different point of view, however, these figures can be regarded as U- or V-shaped curves, that is we can draw tangential lines of any positive or negative slope for the curves. Values for C_1 and C_2 calculated from the broken lines in *Figures 7* and *8* are given in *Table 2*. Comparing $\partial W/\partial I_1$ and $\partial W/\partial I_2$ in *Figure 5* with C_1 and C_2 in *Table 2* for unfilled NR, C_1 is slightly smaller than $\partial W/\partial I_1$ and C_2 is much larger than $\partial W/\partial I_2$. In carbon black filled NR, particularly as filler content increases, both C_1 and C_2 are different from $\partial W/\partial I_1$ and $\partial W/\partial I_2$, respectively. These results indicate that it is nearly impossible to estimate $\partial W/\partial I_1$ and $\partial W/\partial I_2$ from C_1 and C_2 given by the Mooney–Rivlin plot for rubber vulcanizates.

Now we consider why straight lines are shown in *Figures 7* and *8*, despite the fact that both $\partial W/\partial I_1$ and $\partial W/\partial I_2$ are a complicated function of λ and different from C_1 and C_2 in absolute values. As explained before, the Mooney–Rivlin equation, equation (14), is identical

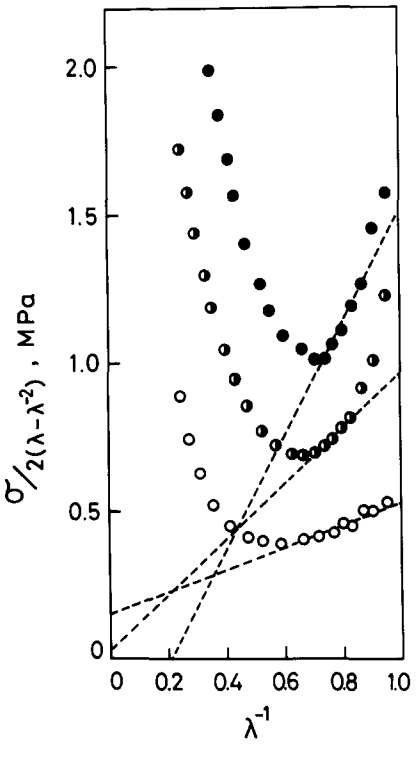

Figure 8 As in *Figure 7*: (○) NR4; (◑) NR6; (●) NR7

Table 2 Mooney–Rivlin constants C_1 and C_2

	C_1 (MPa)	C_2 (MPa)
NR1	0.10	0.11
NR2	0.18	0.12
NR3	0.28	0.15
NR4	0.23	0.25
NR6	0.017	0.98
NR7	−0.20	1.66

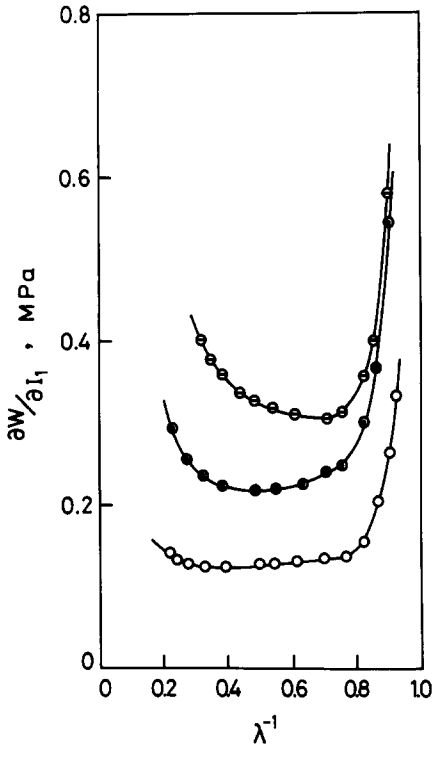

Figure 9 $\partial W/\partial I_1$ as a function of λ^{-1}: (○) NR1; (⊙) NR2: (⊖) NR3

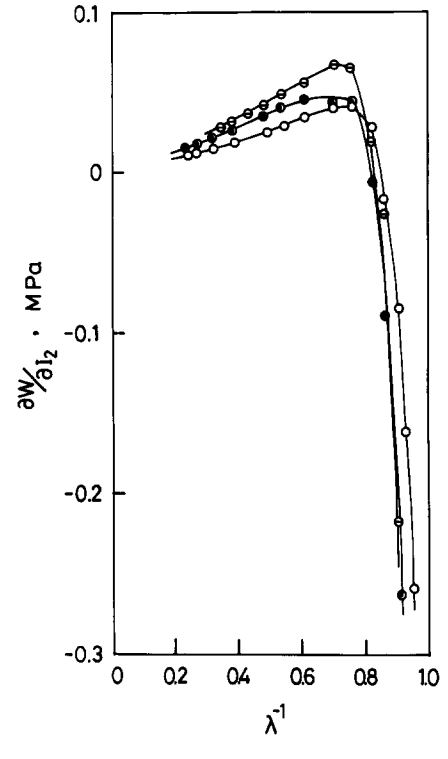

Figure 10 $\partial W/\partial I_2$ as a function of λ^{-1}: (○) NR1; (⊙) NR2; (⊖) NR3

to the general equation (9), which means that the reduced stress σ^* in equation (14) equals $\partial W/\partial I_1 + \lambda^{-1}\partial W/\partial I_2$ in equation (9). That is, the Mooney–Rivlin plot can be reproduced as a plot of $\partial W/\partial I_1 + \lambda^{-1}\partial W/\partial I_2$ as a function of λ^{-1}. *Figures 9–11* are $\partial W/\partial I_1$, $\partial W/\partial I_2$ and $\partial W/\partial I_1 + \lambda^{-1}\partial W/\partial I_2$ plotted against λ^{-1} for unfilled NR. *Figure 11* is fundamentally equal to *Figure 7*. The corresponding plots for filled NR are given in *Figures 12–14*. The agreement between *Figures 14* and *8* is satisfactory. These experimental results show that the Mooney–Rivlin plot can be estimated with the plots in *Figures 11* and *14* independently obtained in strip biaxial testing. We can now derive the answer to the earlier question by analysing straight lines observed in *Figures 11* and *14*. Considering the difficulty of finding

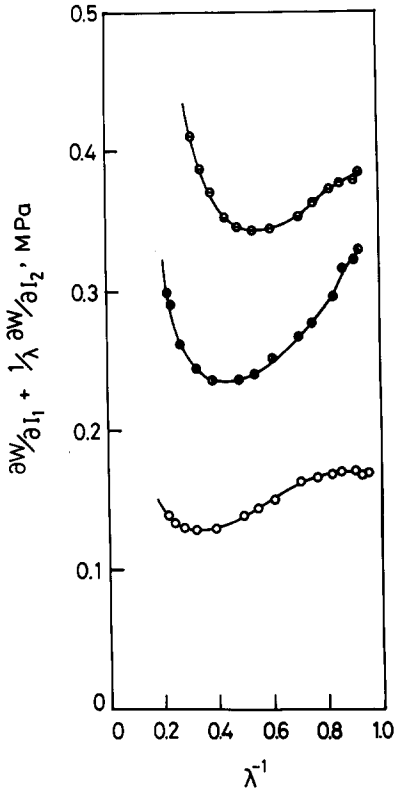

Figure 11 $\partial W/\partial I_1 + \lambda^{-1}\partial W/\partial I_2$ as a function of λ^{-1}: (○) NR1; (⊙) NR2; (⊖) NR3

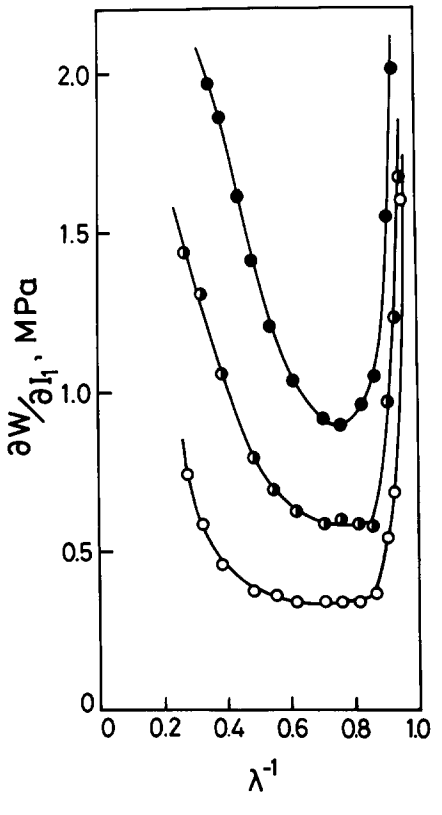

Figure 12 As in *Figure 9*: (○) NR4; (◑) NR6; (●) NR7

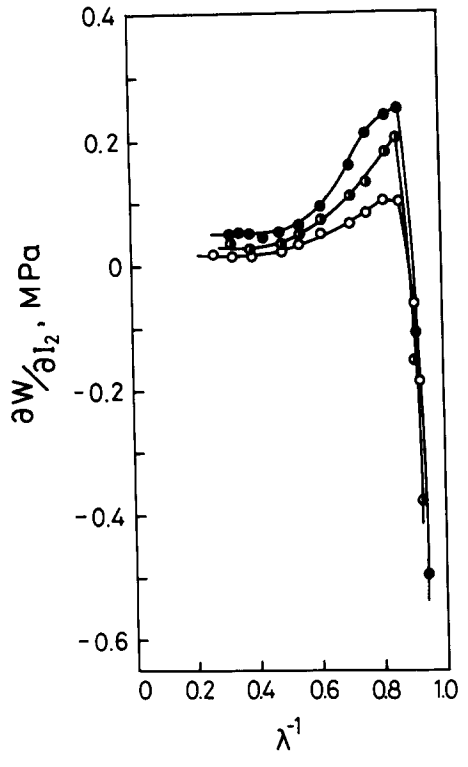

Figure 13 As in *Figure 10*: (○) NR4; (◑) NR6; (●) NR7

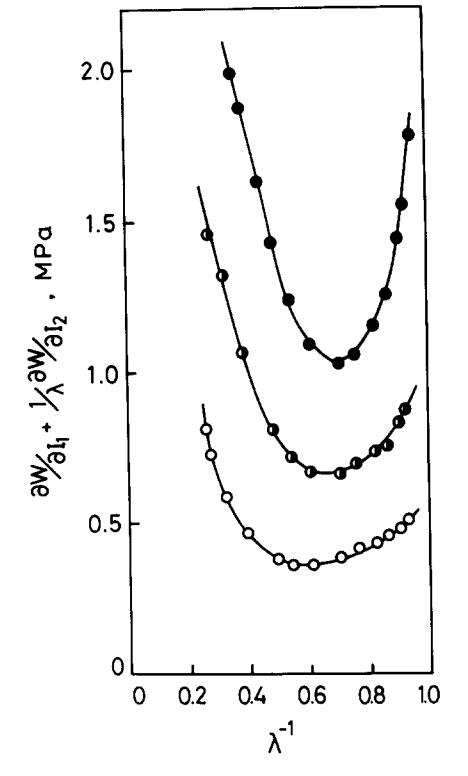

Figure 14 As in *Figure 11*: (○) NR4; (◑) NR6; (●) NR7

a region where $\partial W/\partial I_1$ and $\partial W/\partial I_2$ are constant simultaneously, we can roughly draw the following schematic features for $\partial W/\partial I_1$, $\partial W/\partial I_2$ and $\partial W/\partial I_1 + \lambda^{-1}\partial W/\partial I_2$, where the λ^{-1} axis is divided into three parts, regions I, II and III. Since $\partial W/\partial I_1$ has a U shape as a function of λ^{-1}, $\partial W/\partial I_1$ can be illustrated as in *Figure 15a*, i.e. $\partial W/\partial I_1$ decreases rapidly in region I, keeps nearly constant in region II and increases drastically again with increasing λ^{-1}. The bottom horizontal of the U shape becomes narrow as sulphur or filler contents increase. $\partial W/\partial I_2$ as a function of λ^{-1}, on the other hand, increases linearly in regions I and II and decreases drastically with increasing λ^{-1} (*Figure 15b*). As a result, $\partial W/\partial I_1 + \lambda^{-1}\partial W/\partial I_2$ *versus* λ^{-1} curves will have the form shown in *Figure 15c*. In region I, the contribution of $\partial W/\partial I_2$, then $\lambda^{-1}\partial W/\partial I_2$ to $\partial W/\partial I_1 + \lambda^{-1}\partial W/\partial I_2$ is negligibly small, then $\partial W/\partial I_1 + \lambda^{-1}\partial W/\partial I_2 \approx \partial W/\partial I_1$. Since we can write $\partial W/\partial I_1 \approx k_1$, $\partial W/\partial I_2 \approx \lambda^{-1}k_2$ in region II, then $\partial W/\partial I_1 + \lambda^{-1}\partial W/\partial I_2 \approx k_1 + \lambda^{-2}k_2$, where k_1 and k_2 are constant. That is, $\partial W/\partial I_1 + \lambda^{-1}\partial W/\partial I_2$ as a function of λ^{-1} does not give a simple straight line but a curve of secondary degree gradually increasing with increasing λ^{-1} in region II. In region III, $\partial W/\partial I_1 + \lambda^{-1}\partial W/\partial I_2$ gives entirely contingent results as the summation of two drastically changing parameters, one positive and the other negative. Hence, these results cannot be anticipated. These simple but general features tell us that there is no inevitability for the plot of the reduced stress against λ^{-1} to give a straight line. Although only a few materials were tested, it is better to conclude that we must give a perfectly different meaning for the constants C_1 and C_2 obtained through the Mooney–Rivlin plot assuming a straight line to be actually observed, from the strain energy functions, $\partial W/\partial I_1$ and $\partial W/\partial I_2$. Usually, a straight line on the Mooney–Rivlin plot is drawn passing through the latter half of regions II and III, and consequently the slope of the line becomes too large, which gives a much higher value for C_2 compared with $\partial W/\partial I_2$.

Finally, we show two calculations for NR5; one is the stress–strain relation for uniaxial extension with the strain energy function obtained through strip biaxial testing and the other is that for strip biaxial deformation with the Mooney–Rivlin constants obtained in uniaxial extension for slightly filled NR5. The former has already given in reference 7 for the case of uniaxial extension

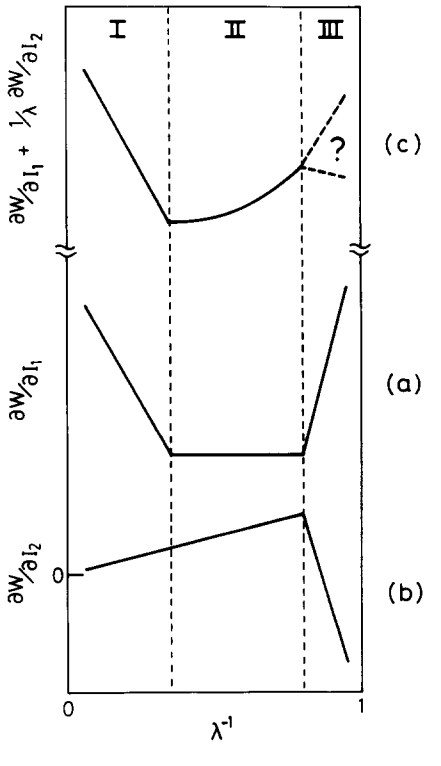

Figure 15 Schematic representation of (a) $\partial W/\partial I_1$, (b) $\partial W/\partial I_2$ and (c) $\partial W/\partial I_1 + \lambda^{-1}\partial W/\partial I_2$ as a function of λ^{-1}

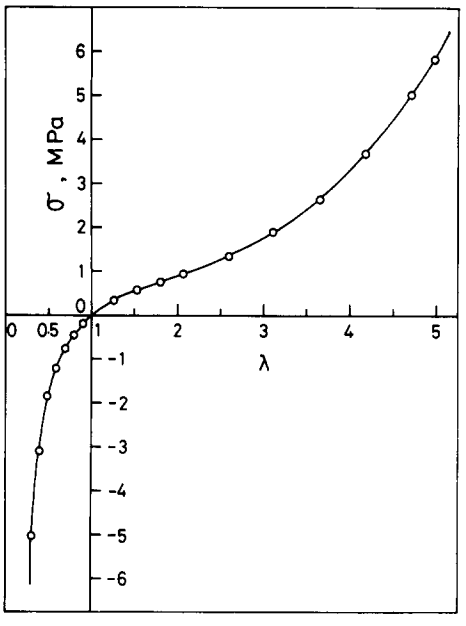

Figure 16 Stress–strain ratio relations in uniaxial extension and compression: (○) experimental data; (—) calculated data with the strain–energy function obtained in a strip biaxial test

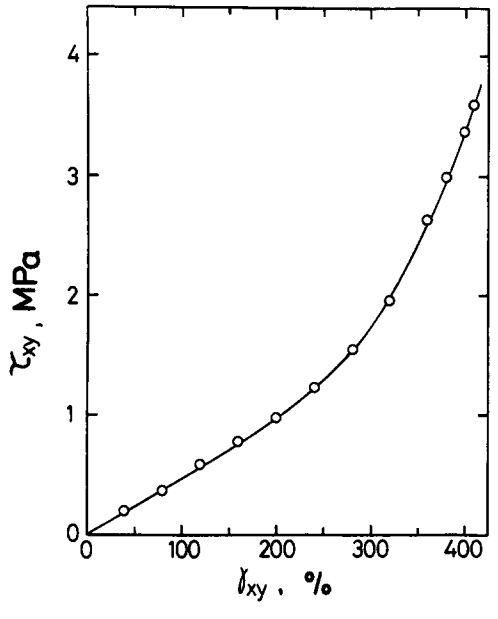

Figure 17 Stress–strain relations in simple shearing; (○) experimental data; (—) calculated data

and compression (*Figure 16*) and simple shearing (*Figure 17*), the agreement between calculation and experiment being excellent. In the latter, calculation is performed for strip biaxial deformation using $C_1 = 0.095$ MPa and $C_2 = 0.228$ MPa (*Figure 18*). It is clearly shown that the calculated results in *Figure 18* differ greatly from the experimental results, in particular, giving opposite results for the relation of σ_1 to σ_2 under large deformation. This discrepancy comes from the general tendency that the value of C_2 obtained from a straight line on the Mooney–Rivlin plot is much larger than $\partial W/\partial I_2$.

CONCLUSIONS

Partial derivatives of the strain energy function, $\partial W/\partial I_1$ and $\partial W/\partial I_2$, of rubber vulcanizates have typical features

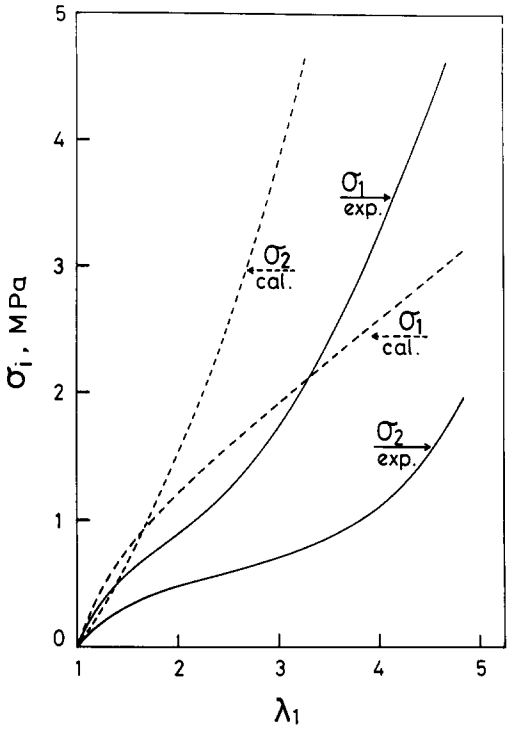

Figure 18 Stress–extension ratio relations in strip biaxial conditions: (—) experimental; (---) calculated with the Mooney–Rivlin constants C_1 and C_2

varying with strain invariant I_1 which are scarcely affected by species, being unfilled and filled. $\partial W/\partial I_1$ decreases rapidly at first then increases again gradually after passing the minimum as I_1 increases. $\partial W/\partial I_2$ behaves conversely to $\partial W/\partial I_1$ with increasing I_1, the ratio of $\partial W/\partial I_2$ to $\partial W/\partial I_1$ being 1/5–1/10.

The Mooney–Rivlin plot is reproduced with the plot of the original equation, equation (9), i.e. the plot of $\partial W/\partial I_1 + \lambda^{-1}\partial W/\partial I_2$ against λ^{-1}. We cannot find any inevitability for the plot to give a straight line. Therefore, even if a straight line is seen, the constants C_1 and C_2 are different from $\partial W/\partial I_1$ and $\partial W/\partial I_2$, respectively. In particular, the most significant problem is the difference between the values of C_2 and $\partial W/\partial I_2$, C_2 being much larger than $\partial W/\partial I_2$.

ACKNOWLEDGEMENT

We wish to extend our sincerest thanks to Professor Kawabata, University of Kyoto, Japan for his helpful advice for designing the apparatus and for constructive discussions.

REFERENCES

1 Rivlin, R. S. *Phil. Trans. R. Soc.* 1948, **A241**, 379
2 Eringen, A. C. 'Nonlinear Theory of Continuous Media', McGraw-Hill, New York, 1962
3 Rivlin, R. S. *Phil. Trans. R. Soc.* 1949, **A242**, 173
4 Treloar, L. R. G. 'The Physics of Rubber Elasticity', 3rd Edn, Clarendon Press, London, 1975, p. 59
5 Rivlin, R. S. and Saunders, D. W. *Phil. Trans. R. Soc.* 1951, **A243**, 251
6 Kawabata, S., Matsuda, M., Tei, K. and Kawai, H. *Macromolecules* 1981, **14**, 154
7 Seki, W., Fukahori, Y., Iseda, Y. and Matsunaga, T. *Rubber Chem. Technol.* 1987, **60**, 856